Pharmaceutical Sciences and Drug Design
ISSN: 3062-4428
2026, Volume 6, Issue 1, Page No: 230-248

Available online at: www.galaxypub.co/page/journals

Galaxy Publication

Cationic Leciplex Nanocarriers for Oral Delivery of Vancomycin Hydrochloride: Design Optimization and Pharmacokinetic Evaluation

Jinwoo Park[1]*, Minji Kim[1], Seung Lee[2]

[1]Department of Pharmaceutical Sciences and Drug Systems, College of Pharmacy, Seoul National University, Seoul, South Korea.
[2]Department of Drug Design Engineering, Faculty of Engineering, KAIST, Daejeon, South Korea.

***E-mail** ✉ jinwoo.park@outlook.com

Received: 19 February 2026; **Revised:** 12 May 2026; **Accepted:** 14 May 2026

ABSTRACT

The aim was to examine how the cationic nanocarrier leciplex (LPX) could boost the oral bioavailability of vancomycin hydrochloride (VAN) through enhancement of its permeation across the intestinal wall. A D-optimal design was employed to evaluate the impact of several variables—namely, lipid molar ratio, cationic surfactant molar ratio, cationic surfactant type, and lipid type—on the attributes of LPX, such as entrapment efficiency (EE%), particle size (P.S.), polydispersity index (P.I.), zeta potential (Z.P.), and steady-state flux (Jss). The optimal formulation underwent additional characterization of morphological features, ex vivo permeation, storage stability, cytotoxicity, and in vivo pharmacokinetics. The optimal LPX displayed a spherical configuration, registering an E.E. of 85.2 ± 0.95%, a P.S. of 52.74 ± 0.91 nm, a P.I. of 0.21 ± 0.02, a Z.P. of + 60.8 ± 1.75 mV, and a Jss of 175.03 ± 1.68 µg/cm²/h. Compared with the plain drug solution, the formulation increased VAN's intestinal permeation by 2.3-fold. The system also proved to be stable, exhibited strong mucoadhesive behavior, and was well accepted via the oral route. The in vivo pharmacokinetic assessment revealed that, compared with the drug solution, VAN's Cmax increased 2.99-fold and its AUC0-12 increased 3.41-fold. Collectively, these results underscore the capability of LPX to elevate the oral bioavailability of drugs with inherently poor absorption.

Keywords: Cationic nanocarriers, Oral bioavailability, Vancomycin hydrochloride, Intestinal permeability, Leciplex, BCS class III

How to Cite This Article: Park J, Kim M, Lee S. Cationic Leciplex Nanocarriers for Oral Delivery of Vancomycin Hydrochloride: Design Optimization and Pharmacokinetic Evaluation. Pharm Sci Drug Des. 2026;6(1):230-48. https://doi.org/10.51847/p78COfv6m5

Introduction

The Biopharmaceutics Classification System (BCS) organizes oral immediate-release medicinal products based on three criteria: solubility in aqueous media, permeation across the intestinal wall, and dissolution behavior [1]. Drugs in BCS Class III, however, tend to be strongly hydrophilic and exhibit weak permeation characteristics [2]. Owing to their very limited oral bioavailability, agents in this category are mostly given by injection—a route often associated with discomfort and, in some cases, significant risk. This class also incorporates therapeutically important molecules, such as peptides and RNA-based pharmaceuticals, creating a pressing need for advanced oral delivery platforms that offer simpler, pain-free administration [3].

Multiple tactics have been tried to enhance intestinal permeability of class III compounds, including encapsulating the active molecule within a shielding particulate vehicle tagged with site-directed ligands or orchestrating the localized delivery of the drug-vehicle assembly [4]. A wide range of carrier systems has consequently emerged to enhance the oral bioavailability of class III agents, including micro- and nanoparticles, nanoemulsions, and formulations containing permeation promoters or hydrophobic ion pairs [5].

Drug uptake from the intestine is driven chiefly by the transcellular route, whereas the paracellular route accommodates only select small hydrophilic molecules [6]. Larger molecules (macromolecules), such as peptides

and RNA-based therapeutics, struggle to enter the portal circulation via the transcellular route. The paracellular option—movement through the aqueous pores of tight junctions—is likewise not viable. Rather, macromolecules undergo swift, efficient transport via M cells, which phagocytose them and shuttle them from the gut lumen into the associated lymphoid tissue. In humans, however, M cells are extremely sparse, accounting for less than 1% of the intestinal lining [7]. These therapeutic payloads also undergo hydrolytic and enzymatic breakdown in the gastrointestinal tract (GIT). Consequently, oral bioavailability for macromolecules remains inherently low.

An oral delivery platform aimed at increasing macromolecule absorption must therefore fulfill several roles: shielding the cargo from hydrolysis and enzyme-driven degradation in the aggressive gastric conditions of the GIT, facilitating uptake across the intestinal barrier, and possessing mucus-interactive features. Formulations that adhere to mucus can lengthen the window for drug uptake in the gut by resisting mucociliary removal. In contrast, those designed to penetrate mucus can speed through the stagnant aqueous boundary to encounter the absorptive epithelium [8].

The scientific literature documents the utility of nanocarriers in increasing the oral bioavailability of water-soluble macromolecules. These systems can trap bioactive macromolecular cargo within their structural framework or central cavity, protecting the degradative lumen of the GIT. Nanocarriers can also be internalized by epithelial cells (via endocytosis or transcellular uptake) or by M cells residing in Peyer's patches [9, 10]. They may also carry permeation enhancers within their structure or be surface-functionalized with ligands to promote oral absorption [11].

Vancomycin hydrochloride (VAN) represents a water-attracting glycopeptide antibiotic possessing a substantial molecular mass of 1485.7 Da. It is used in both preventive therapy and the management of severe, potentially fatal Gram-positive bacterial infections, including those caused by Staphylococcus aureus and related pathogens [12]. VAN was therefore adopted as a representative drug to validate the capacity of nanocarriers to strengthen the oral bioavailability of a macromolecular class III agent.

Delivering VAN by mouth poses considerable challenges, as its oral bioavailability is curtailed by acid-mediated breakdown in the stomach, enzyme-catalyzed degradation in the intestine, poor epithelial barrier permeability, and rapid expulsion from the GIT [13]. An oral formulation engineered to improve VAN absorption must accordingly provide protection against hydrolytic and enzymatic degradation in the GIT, promote intestinal uptake, and sustain the drug's presence in the GIT over an extended period.

Several nanoparticle-based delivery platforms have been explored to boost the oral uptake of VAN, including polymeric carriers, liposomal vesicles, self-emulsifying drug delivery systems (SEDDS), and inorganic nanoparticles. Loveymi *et al*. [14] demonstrated that surfacing VAN nanoparticles with a bioadhesive polymer could prolong gastrointestinal retention and enhance the intimacy between the drug and the absorptive lining, thereby increasing intestinal drug permeation. Zakeri-Milani *et al*. [15] noted that poly (lactide-co-glycolide) nanoparticles released VAN for a markedly longer period than a simple physical blend; additionally, nanoparticle encapsulation was shown to enhance VAN transport across the gut wall. Zaichik *et al*. [16] designed a self-emulsifying drug delivery system (SEDDS) to enhance VAN's lipophilicity via hydrophobic ion-pair formation with cetyltrimethylammonium bromide (CTAB), thereby increasing intestinal permeation. In related work, Efiana *et al*. [17] embedded VAN within SEDDS modified with papain-palmitate, again exploiting hydrophobic ion pairing, to facilitate VAN's passage through intestinal mucus, and observed that incorporating 0.5% papain-palmitate significantly elevated the mucus-penetrating ability of the SEDDS. In a more recent investigation, Ndayishimiye *et al*. [12] developed silica nanoparticle (SNP)-centered formulations to potentiate VAN's traversal of the epithelial layer. The authors found that VAN incorporated into SNPs displayed markedly superior permeation across a cultured epithelial monolayer compared with the plain drug solution. Separately, Uhl *et al*. [18] prepared tetraether lipid-reinforced liposomal nanocarriers adorned with cell-penetrating peptides to heighten VAN's oral bioavailability by promoting its passage through the mucous barrier. The body of prior research confirms that a variety of nanocarrier architectures have been customized to upgrade VAN's oral bioavailability; nonetheless, the pursuit of a platform that is simultaneously amenable to large-scale production, biologically safe, and straightforward to fabricate, while still delivering a commensurate boost in VAN's oral bioavailability, remains critically important.

Published evidence suggests that intestinal permeation promoters or bio-enhancers housed within nanocarriers may potentiate the oral bioavailability of macromolecular drugs via one or a convergence of the following pathways: (a) temporary disruption of epithelial integrity, thereby streamlining drug ingress; (b) increased propensity of lipid-based vesicles to merge with cell membranes; (c) relaxation of tight junction complexes, which

opens the paracellular route to drug transit [19]. Surface-active agents, such as bile salts, cationic amphiphiles, and nonionic surfactants, are widely incorporated into nanocarrier formulations. Among these, cationic surfactants have garnered substantial attention as bio-enhancers by virtue of their capacity to promote both intracellular delivery and mucoadhesive interactions of the nanocarrier [20, 21].

Leciplex (LPX) was identified as a promising candidate to improve the oral bioavailability of VAN, owing to its facile scalability, exclusion of organic solvents, straightforward manufacturing process, and superior stability [22]. LPX represents a cationic, phospholipid-anchored vesicular construct whose fundamental building blocks comprise a phospholipid, a cationic surfactant, and a biocompatible solvent. The decision to employ LPX for magnifying VAN's intestinal permeability rests on its net positive surface charge, which encourages nanocarrier adherence to the negatively charged surfaces of epithelial cells and consequently fosters cellular assimilation of the payload [23]. Earlier reports have also documented the durability of positively charged vesicles under GIT conditions, suggesting that the cationic exterior serves as a protective barrier that prevents bile acids from accessing and disrupting the lipid bilayer [24, 25]. A further perceived asset is the sub-100 nm particle diameter (≤100 nm), which is understood to facilitate transmembrane permeation [26].

In contemporary practice, design of experiments (DOE) methodologies are routinely applied to the formulation and optimization of drug delivery systems, principally because they minimize the total number of experimental trials required. The D-optimal design (DOD), a tool within the response surface methodology family, is particularly advantageous when categorical factors are under investigation; it uncovers main effects and interactions among mixture components while simultaneously reducing the predicted variance across experimental runs [27, 28]. For these reasons, DOD was deployed to systematically probe and contrast the effects of different formulation variables on LPX attributes.

Materials and Methods

Materials

Vancomycin hydrochloride (VAN) was kindly provided by Kahira Pharmaceutical Co. (Cairo, Egypt). Phospholipon 90 G (PL-90 G) was procured from Lipoid GmbH (Ludwigshafen, Germany). Soy phosphatidylcholine (SPC), cetyltrimethylammonium bromide (CTAB), dimethyldidodecylammonium bromide (DDAB), Roswell Park Memorial Institute (RPMI) culture medium, sulforhodamine-B, tris aminomethane base, and mucin were acquired from Sigma-Aldrich Chemical Co. (St. Louis, MO, USA). Transcutol was sourced from Alfa Aesar (Kandel, Germany). All additional chemicals and solvents met analytical grade specifications.

Preparation of VAN-loaded LPX

A single-step fabrication protocol was followed to generate LPX batches exhibiting a range of lipid-to-surfactant molar ratios **(Table 1).** In brief, the lipid and surfactant components were weighed out and dissolved in Transcutol P in a shaking water bath (LWBS-A12, Labtron, Camberley, UK), thermostated at 70 °C until a transparent, yellow, homogeneous solution was obtained. Concurrently, an aqueous phase containing 50 mg of VAN was heated to 70 °C and then introduced in a single pour into the lipid mixture while cyclomixing (~1200 rpm) was maintained, continuing until a homogeneous dispersion was obtained [29].

Table 1. DOD of VAN-loaded LPX.

Variable	High level	Low level
X1: Lipid molar ratio	1	0
X2: Cationic surfactant molar ratio	5	1
X3: Cationic surfactant type	PL-90 G	SPC
X4: Lipid type	DDAB	CTAB

Abbreviations: DOD = D-optimal design, CTAB = Cetrimonium bromide, DDAB = Dimethyldioctadecylammonium bromide, SPC = Soya phosphatidylcholine, and PL-90 G = Phospholipon 90 G.

Characterization of VAN-loaded LPX

Determination of entrapment efficiency (E.E.%)

The E.E.% of VAN was quantified by membrane dialysis. Specifically, a 1 mL aliquot of the LPX formulation was sealed in a dialysis bag (M.W. 12,000–14,000 Dalton) and submerged in a beaker containing 100 mL of distilled water. At scheduled time points, portions of the sample were collected, and the concentration of VAN

was determined spectrophotometrically at 280 nm (UV-1650; Shimadzu Corp., Kyoto, Japan). The E.E. percentage was derived from the relationship shown below [30]:

$$\text{E.E. (\%)} = \frac{\text{Total VAN amount} - \text{Diffused VAN amount}}{\text{Total VAN amount}} \times 100 \quad (1)$$

Determination of particle size, polydispersity index, and zeta potential

The mean hydrodynamic diameter (z-average), P.I., and interfacial charge of the LPX dispersions were evaluated by Dynamic Light Scattering (DLS) on a Malvern Zetasizer NanoZS instrument (Zetasizer Nano Series, Malvern, UK) operated at 25 °C. Immediately before the measurements, each sample was diluted with double-distilled water to attain a suitable scattering intensity [31].

In vitro drug release study

The in vitro liberation profile of VAN from the LPX formulations was monitored using Franz-type diffusion cells. The release environment consisted of phosphate buffer (PBS, pH 7.4). A cellulose membrane (molecular weight cut-off 12,000 Da) was hydrated in distilled water for a 12 h period preceding the experiment. The donor compartment received 2 mL of the LPX dispersion (containing 10 mg VAN). The receptor compartment was charged with 50 mL of release medium, held at 37 °C, and agitated at 50 rpm. At defined intervals, 0.5 mL samples were withdrawn from the receptor and promptly replaced with an identical volume of fresh, pre-warmed medium. The VAN content of these samples was quantified by UV spectrophotometry at 280 nm. The total quantity of VAN released was charted as a function of time, and the steady-state flux (Jss; µg/cm²/h) was computed from the gradient of the linear region of this plot [32]. To interpret the release mechanism, the experimental data were fitted to several kinetic models—namely, zero-order, first-order, Higuchi, and Korsmeyer-Peppas. The most appropriate model was selected based on the highest correlation coefficient (R^2).

Optimization of VAN-loaded LPX formulations

A D-optimal experimental matrix was constructed and analyzed with the aid of Design Expert® software version 7 (Stat Ease, Inc., Minneapolis, MN, USA) to probe the consequences of several formulation variables on LPX attributes. The four independent factors incorporated into the LPX experimental layout were (X1: lipid molar ratio), (X2: cationic surfactant molar ratio), (X3: cationic surfactant type), tested at two distinct levels, and (X4: lipid type) similarly examined at two levels. The set of response variables tracked for the study comprised E.E.% (Y1), P.S. (Y2), P.I. (Y3), Z.P. (Y4), and Jss (Y5).

Selecting the optimized VAN-LPX formula

The desirability function, a tool for simultaneously balancing multiple responses, was applied to pinpoint the optimal formulation. The decision rule guiding the selection process stipulated that the optimized formula should deliver the lowest possible P.S. and P.I. while attaining the highest achievable Jss, EE%, and Z.P.

Morphology of the optimized VAN-LPX formula

The physical form and surface architecture of the LPX nanocarrier were examined by transmission electron microscopy (TEM) (JEM-1230, Joel, Tokyo, Japan) after negative staining [31].

Ex Vivo permeation study via non-everted intestinal sac model

A segment of intestine was isolated following a midline abdominal incision on a sacrificed rabbit. The interior of the excised sac was washed by repeatedly flushing Ringer's solution through its lumen until all visible traces of fecal debris were eliminated. One terminus of the intestinal segment was then tied off, exercising caution to avoid tissue injury. A volume of 0.5 mL of either the plain VAN solution or the test formulation (equivalent to 2.5 mg of VAN) was carefully introduced into the rabbit gut sac using a micropipette, after which the opposite opening was also securely ligated. The loaded sac was subsequently placed in a vessel containing 20 mL of Ringer's solution, which was thermostated at 37 °C. At scheduled sampling intervals, 0.5 mL was drawn from the receiver compartment and replaced with an identical volume of fresh, pre-warmed medium. The concentration of VAN that had traversed the intestinal wall was quantified by HPLC, utilizing a C18 stationary phase and a mobile phase blend consisting of citrate buffer (pH 4), acetonitrile, and methanol combined in an 85:10:5 (v/v/v) proportion,

pumped at 1.0 mL/min with ultraviolet detection set to 280 nm. The apparent permeability coefficient was derived as the mass of VAN (µg) transported per unit area of mucosal surface (cm²), in accordance with the following expression [33]:

$$\text{Apparent permeability} = \frac{\Delta Q}{\Delta t \times A \times C_0} \ (\text{cm/h}) \quad (2)$$

where ΔQ/Δt signifies the transport rate across the intestinal sac (µg/h), A denotes the surface area of the sac (cm²), and C_0 corresponds to the starting drug concentration in the donor compartment (µg/mL). ΔQ represents the cumulative amount of drug permeated (µg/cm²).

Differential scanning calorimetry

The thermal transition profiles of the isolated LPX constituents and of the finalized LPX formulation were characterized using differential scanning calorimetry (DSC 204 F1, Netzsch, Germany). Specimens were precisely weighed into conventional aluminum crucibles. Thermograms were collected during heating and cooling sweeps at a ramp rate of 10 °C min^{-1} over a temperature range of 25 to 300 °C.

Effect of storage on the selected LPX formula

The physical resilience of the LPX formulation was appraised to confirm its ability to maintain its colloidal dimensions and surface charge during shelf storage. The preparation was held at 4 °C for 3 months, after which its P.S., P.I., and Z.P. were remeasured and compared with the values recorded for a freshly manufactured equivalent. Furthermore, the capacity of the LPX formulation to withstand enzyme-driven degradation was examined in simulated gastric fluid (SGF) and simulated intestinal fluid (SIF) at 37 °C. Because the ultra-fine size of the LPX dispersion rendered direct separation from the incubation fluids impracticable, an alternative procedure was devised to estimate the proportion of VAN safeguarded after contact with SGF and SIF. Specifically, 1 mL of the formulation was blended with either 1 mL of SGF or 1 mL of SIF, transferred into a dialysis bag, sealed, and immersed in 100 mL of distilled water for 2 h under constant stirring at 100 rpm. At the conclusion of this interval, a 0.5 mL aliquot was withdrawn from the external aqueous phase and analyzed by UV spectrophotometry at 280 nm to determine the amount of drug retained in the formulation under the differing pH conditions.

Evaluation of mucoadhesion properties of the selected formula

The propensity of the manufactured LPX to adhere to mucosal surfaces was gauged by monitoring its electrostatic association with negatively charged mucin glycoproteins. In practice, an aqueous mucin dispersion was formulated and subsequently combined with the LPX preparation at a 1:1 volumetric ratio at 37 °C. The resultant Z.P. of the mixed systems was then recorded using a Zetasizer Nano Z.S. instrument (Malvern Instruments Ltd., UK) [30].

Cytotoxicity assay

A human colorectal adenocarcinoma epithelial cell line (CaCo-2) was sourced from Nawah Scientific Inc. (Mokatam, Cairo, Egypt). The cells were propagated in Roswell Park Memorial Institute (RPMI) culture medium fortified with 100 mg/mL streptomycin, 100 units/mL penicillin, and 10% heat-inactivated fetal bovine serum, within a humidified incubator maintained at 37 °C under a 5% (v/v) CO_2 atmosphere. Cellular viability was evaluated using the sulforhodamine B (SRB) colorimetric assay in 96-well microplates. In outline, cells were seeded at a density of 5×10^3 cells per well and incubated overnight to permit attachment, after which they were challenged with the designated concentrations of the various test formulations for a 72 h exposure window. Fixation was accomplished by discarding the culture supernatant and adding 150 µL of 10% trichloroacetic acid (TCA) to each well, followed by cold storage at 4 °C for 1 h. The TCA solution was then removed, and the plates were rinsed with purified water and left to air-dry. Thereafter, 70 µL of SRB staining solution was added to each well, and the mixture was incubated in the dark at room temperature for 30 min. Excess dye was eliminated by rinsing the plates with 1% acetic acid, and the plates were dried in air overnight. The protein-bound SRB stain was subsequently extracted using 150 µL of tris aminomethane base (10 mM), with the plates placed on a shaker for 5 min to ensure complete solubilization. Optical density was recorded at a wavelength of 540 nm on a BMG LABTECH®-FLUOstar Omega microplate reader (Ortenberg, Germany) [34].

In vivo assessment of the selected LPX formula

Ethical clearance for the animal experiments was granted by the Research Ethics Committee of the Faculty of Pharmacy at Cairo University (Approval no. PI 2842). Every animal procedure was performed in full conformity with the Animal Research: Reporting of In Vivo Experiments (ARRIVE) standards.

Twenty-four male Wistar albino rats, each having a body mass of 200 ± 20 g, were sourced from the breeding facility operated by the Faculty of Veterinary Medicine, Cairo University. Throughout the study, strict compliance with all established principles of laboratory animal husbandry and welfare was maintained. The animals were accommodated in cages within a climate-monitored room set at 25 ± 2 °C and 50−60% relative humidity, subjected to alternating 12 h periods of light and darkness. Drinking water was supplied ad libitum, whereas solid feed was withheld for a 24 h fasting window before the dosing day. The rat cohort was randomly split into two groups, each containing 12 individuals: Group 1 received the drug in aqueous dispersion, and Group 2 received the optimized LPX formulation. Both treatments were administered orally at a single dose of 20 mg/Kg [35]. Under light ether sedation, serial blood draws (0.5 mL per sample) were collected into heparinized plastic centrifuge tubes through capillary glass tubing measuring 0.8–1.1 mm in diameter at the following post-administration intervals: 0.5, 1, 2, 3, 4, 5, 6, 7, 8, and 12 h. Following centrifugation, a 200 µL fraction of harvested plasma was aspirated with a pipettor and vortex-mixed together with an identical volume of methanol to induce protein precipitation. This blend was agitated in a vortex apparatus for 90 s and then spun at 9000 rpm for 10 min. A sample of the resulting clear supernatant (20 µL) was subsequently assayed using a validated HPLC protocol [12]. The plasma concentration-versus-time profiles obtained for VAN were processed using non-compartmental pharmacokinetic modeling in Kinetica (version 4.4.1). The maximal recorded plasma concentration (Cmax) together with the time point of its appearance (Tmax) were extracted directly from the empirical concentration-time data. Computation of the area beneath the plasma concentration-time curve from the zero timepoint up to the final measurable sampling time (AUC0–t) employed the linear trapezoidal summation method. The mean residence time (MRT) was also derived. Between-group statistical evaluation relied on the unpaired, two-tailed t-test.

Statistical analysis of data

All statistical computations were conducted using the GraphPad Instat software package (version 3.1, Dotmatics, Boston, MA, USA). Data are expressed as the mean ± S.D. Comparative statistical assessments were undertaken using the t-test and one-way analysis of variance (ANOVA) supplemented by the Tukey post-hoc test, with the significance threshold fixed at $P < 0.05$.

Results and Discussion

Design optimization

A standard LPX construct is built on a foundation of phospholipid and a cationic agent blended in a particular ratio as its essential structural elements. In this investigation, multiple preparations were manufactured using differing ratios and distinct chemical variants of both the phospholipid and surfactant constituents. These LPX batches were subsequently characterized to determine the influence of the independent experimental factors on the measured outcome variables, as shown in **Table 2**. The statistical outputs generated from the design analysis are collated in **Table 3**.

Table 2. Experimental runs, independent variables, and measured response of the DOD of VAN-loaded LPX.

Formulation code	Surfactant molar ratio (X_2)	Lipid molar ratio (X_1)	Lipid type (X_4)	Surfactant type (X_3)	Jss (µg/cm²/h) (Y_5)	Z.P. (mV) (Y_4)	P.I. (Y_3)	P.S. (nm) (Y_2)	E.E.% (Y_1)
F1	0	5	SPC	DDAB	36.05 ± 0.49	−64.4 ± 0.55	0.26 ± 0.008	194.5 ± 1.75	99.33 ± 1.5
F2	0.5	2	PG90	DDAB	166.23 ± 0.55	57.1 ± 1.1	0.29 ± 0.002	28.32 ± 1.15	81.6 ± 1.8
F3	1	1	PG90	DDAB	187.41 ± 1.20	64.9 ± 0.45	0.19 ± 0.005	18.51 ± 0.77	75.6 ± 1.2

F4	1	5	PG90	CTAB	102.61 ± 0.42	55.9 ± 1.35	0.40 ± 0.025	156.0 ± 1.59	94.0 ± 1.5
F5	0	3	SPC	CTAB	136.08 ± 0.05	−52.9 ± 0.89	0.26 ± 0.005	96.48 ± 1.24	93.3 ± 1.1
F6	1	5	PG90	DDAB	156.0 ± 0.96	52.3 ± 0.96	0.23 ± 0.043	147.0 ± 0.94	90.9 ± 0.78
F7	0.5	3	SPC	DDAB	102.15 ± 1.10	−29.3 ± 0.35	0.24 ± 0.010	68.47 ± 0.85	94.4 ± 0.60
F8	0	3	PG90	DDAB	113.28 ± 1.19	10.5 ± 1.20	0.51 ± 0.020	103.0 ± 0.55	88.2 ± 1.0
F9	0	5	SPC	DDAB	37.72 ± 0.89	−66.8 ± 0.41	0.24 ± 0.018	189.3 ± 1.75	96.99 ± 1.7
F10	0	1	PG90	CTAB	142.98 ± 0.69	19.8 ± 0.25	0.31 ± 0.028	102.2 ± 2.1	92.0 ± 1.7
F11	1	1	SPC	CTAB	178.44 ± 0.31	33.6 ± 0.30	0.28 ± 0.018	49.17 ± 0.28	91.2 ± 1.4
F12	1	5	SPC	CTAB	141.25 ± 0.17	−33.2 ± 1.4	0.26 ± 0.051	121.2 ± 0.66	96.8 ± 1.41
F13	1	1	SPC	DDAB	133.72 ± 0.5	42.3 ± 0.95	0.33 ± 0.030	73.85 ± 1.35	91.9 ± 0.81
F14	0	1	SPC	DDAB	58.37 ± 0.26	−49.4 ± 0.6	0.26 ± 0.002	148.4 ± 0.22	95.6 ± 1.3
F15	0.5	2	SPC	CTAB	160.69 ± 0.48	22.1 ± 1.05	0.34 ± 0.008	83.54 ± 1.23	95.0 ± 1.1
F16	0	5	PG90	CTAB	76.63 ± 0.45	3.05 ± 0.19	0.41 ± 0.046	162.4 ± 1.30	93.4 ± 1.2
F17	0	1	PG90	CTAB	142.98 ± 0.69	19.8 ± 0.15	0.31 ± 0.022	102.2 ± 1.69	89.6 ± 1.9
F18	0.5	3	PG90	CTAB	149.63 ± 0.43	38.2 ± 0.65	0.38 ± 0.005	61.7 ± 1.35	87.2 ± 1.3
F19	1	5	PG90	DDAB	161.24 ± 0.16	50.6 ± 0.25	0.35 ± 0.001	140 ± 1.52	91.4 ± 1.9

Abbreviations: E.E.% = entrapment efficiency percentage; P.S. = particle size; P.I. = polydispersity index; Z.P. = zeta potential; Jss = steady-state flux, LPX = leciplex.

Table 3. Output data of the DOD analysis of LPX formulations and predicted and observed values for the selected LPX formula.

Source	E.E.% (Y1)	P.S. (nm) (Y2)	P.I. (Y3)	Z.P. (mV) (Y4)	Jss (μg/cm²/h) (Y5)
Probability value	<0.0001	0.0016	0.1982	< 0.0001	< 0.0001
Model type	2 FI	Quadratic	-	Linear	Quadratic
X1 = A = Proportion of lipid	< 0.0001	0.0004	0.0962	0.0008	< 0.0001
X2 = B = Proportion of surfactant	0.0381	0.0043	0.2669	<0.0001	< 0.0001
X3 = C = Class of surfactant	0.3271	0.8949	0.9691	0.5983	< 0.0001
X4 = D = Class of lipid	< 0.0001	0.1166	0.1360	< 0.0001	< 0.0001
Signal-to-noise ratio	19.724	10.43	4.53	19.791	42.568
Coefficient of determination (R^2)	0.9636	0.84	0.33	0.9132	0.9969
Modified R^2	0.9226	0.76	0.14	0.8884	0.9907
Forecast R^2	0.8496	0.6	−0.26	0.8332	0.9044
Influential variables	X1, X2, X4	X1, X2	-	X1, X2, X4	X1, X2, X3, X4
Forecast the result of the chosen formulation	87.38	50.98	0.22	65.1	178.41
Actual result of the chosen formulation	85.20 ± 0.95	52.74 ± 0.91	0.21 ± 0.02	60.8 ± 1.75	175.03 ± 1.68

Fitted model equation	+91.50 + 3.47×A − 1.23×B + 0.44×C − 3.84×D + 1.92×A×B − 1.48×A×C + 1.34×A×D + 0.27×B×C + 0.95×B×D + 1.61×C×D	+106.80 + 43.44×A − 21.6×B − 2.16×C − 6.84×D	-	+126.49 − 20.74×A + 23.12×B + 8.84×C + 7.92×D + 1.58×A×B + 6.16×A×C − 5.24×A×D − 12.03×B×C − 3.62×B×D − 20.32×C×D

Abbreviations: E.E.% = entrapment efficiency percentage; P.S. = particle size; P.I. = polydispersity index; Z.P. = zeta potential; Jss = steady-state flux.

Effect of formulation variables on the entrapment efficiency%

Quantification of E.E.% across the LPX series was performed using the dialysis method. In this procedure, unencapsulated drug molecules are free to migrate outward across the membrane into the surrounding aqueous phase, whereas the entrapped payload remains sequestered inside the vesicles until its eventual liberation from the carrier. **Figure 1** shows that the independent variables X1, X2, and X4 each exert a meaningful impact on the E.E.% of VAN in the LPX dispersions. According to **Table 2**, the E.E.% values for the VAN LPX formulations ranged from 75.6 ± 1.2% to 99.33 ± 1.5%. The statistical output confirmed that the lipid molar ratio (X1) had a highly significant bearing on E.E.% ($P < 0.0001$). This trend aligns with the observations of Date *et al*. [36], who reported that increasing the lipid content of the formulation increased E.E.% by promoting the assembly of vesicles with enhanced structural rigidity, thereby improving their capacity to contain hydrophilic drug payloads and suppress outward diffusion.

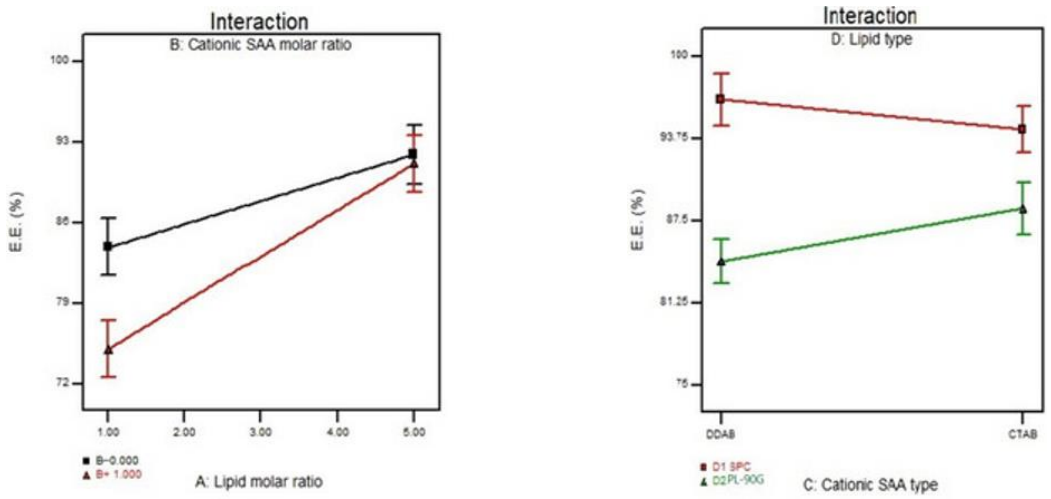

a) b)

Figure 1. The effect of lipid molar ratio (X1), cationic surfactant molar ratio (X2), cationic surfactant type (X3), and lipid type (X4) on E.E.%. Abbreviation: E.E.% = entrapment efficiency percent.

In the opposite direction, raising the level of the cationic surfactant component led to a decline in E.E.% ($P = 0.0381$). A plausible explanation for this observation lies in the detergent-like properties of the surfactant, which solvate phospholipid molecules, thereby compromising vesicle membrane cohesion and allowing the entrapped drug to leak from the LPX carriers. This outcome is consistent with the report by Salama *et al*. [37], who noted a marked decrease in spironolactone encapsulation efficiency as the surfactant fraction increased. The identity of the lipid (X4) likewise emerged as a highly significant factor ($P < 0.0001$) governing E.E.%, with maximum entrapment values consistently occurring in LPX built from SPC as opposed to PL-90 G. This divergence may be traced to fundamental structural distinctions between the two lipid species: SPC incorporates a share of saturated fatty acyl chains and thus organizes into a densely packed, rigid architecture that resists drug escape from the LPX structures. PL-90 G, by comparison, is composed largely of unsaturated fatty acid residues, which produce a more fluid and less ordered matrix that inadvertently facilitates the outward passage of hydrophilic drugs from the

nanocarriers. These findings echo those of Eroğlu *et al*. [38], who concluded that unsaturated phospholipids are more pliable and, consequently, present a weaker barrier to drug retention within the lipid bilayer. An additional factor that may contribute to the disparity in E.E.% between the two lipid types is the difference in their inherent surface charge, which is especially relevant for a positively charged drug such as VAN. At neutral pH, SPC carries a net anionic character, whereas PL-90 G is approximately electroneutral. It was therefore reasonable to expect LPX prepared with SPC to record superior E.E.% values, driven by the electrostatic attraction operating between the negatively charged phospholipid (SPC) and the positively charged drug (VAN) [39].

Effect of formulation variables on the particle size

The diameter of nanocarriers profoundly influences their ability to cross the intestinal wall, as smaller particles more readily facilitate drug transport via endocytic uptake and the paracellular route. According to the data compiled in **Table 2**, the P.S. measurements for the LPX batches fell within the bounds of 18.51 ± 0.77 and 194.50 ± 1.75 nm. Statistical evaluation via ANOVA confirmed that factors X1 and X2 each significantly influenced the P.S. of the cationic nanocarrier, as shown in **Figure 2**. Enriching the lipid fraction led to progressively larger vesicular structures. This finding aligns with the E.E.% results, in which increasing the lipid molar ratio substantially elevated the sequestration of the water-soluble drug and, in turn, generated vesicles of greater volume. The addition of a cationic surfactant to the LPX mixtures, conversely, triggered a sharp contraction in P.S., which may be credited to the steric barrier erected by surfactant molecules that discourages or suppresses vesicle clustering. An alternative explanation involves a lowering of the interfacial tension at the aqueous–lipid boundary, a condition conducive to the emergence of smaller vesicles, or surfactant-mediated lipid dissolution that permits drug egress from the LPX and consequently shrinks the P.S. These patterns resonate with the account by Khatoon *et al*. [40], who reported that elevated surfactant levels paired with meager phospholipid content gave rise to vesicles of diminished stature.

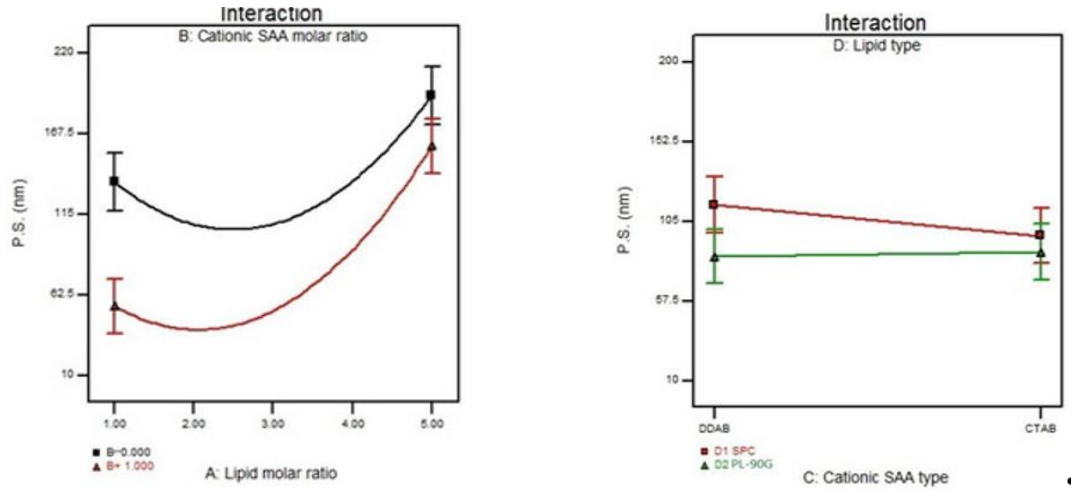

a) b)

Figure 2. The effect of lipid molar ratio (X1), cationic surfactant molar ratio (X2), cationic surfactant type (X3), and lipid type (X4) on P.S. Abbreviation: P.S. = particle size.

Effect of formulation variables on the polydispersity index

The P.I. readings registered for every LPX dispersion remained beneath the 0.5 threshold. Upon scrutiny of the relationship between the independent variables and P.I. (Y3), no statistically robust model emerged from the dataset.

Effect of formulation variables on the zeta potential

The Z.P. parameter is customarily employed as a gauge for estimating the colloidal stability of a dispersed system. As laid out in **Table 2**, the Z.P. magnitudes recorded for the LPX formulations covered a spectrum extending from −66.8 ± 0.41 to + 64.9 ± 0.45 mV. The Z.P. of the as-prepared LPX was demonstrably shaped by X1, X2, and X4, as portrayed in **Figure 3**. The lipid molar ratio (X1) commanded a strong influence over Z.P.; by way of illustration, LPX batch F5, which consisted solely of SPC and cationic surfactant at a 3:0 ratio, exhibited a Z.P.

of −52.9 ± 0.89 mV, yet elevating that ratio to 5:0 in formulation F1—while retaining the identical phospholipid variety—caused the measurement to shift more sharply negative to −66.8 ± 0.41 mV. The inclusion of a cationic surfactant in the LPX assemblies modulated the Z.P. by progressively offsetting the vesicles' inherent electronegativity. The deliberate engineering of a net positive surface charge in these formulations was intended to amplify electrostatic adhesive forces between the cationic LPX and the negatively charged mucus gel layer, thereby enhancing mucoadhesive anchoring of the LPX nanoparticles. Such an effect could conceivably extend gut retention and sustain drug presentation to the underlying absorptive epithelium. In a similar vein, raising the molar fraction of surfactant (X2) propelled the Z.P. toward increasingly electropositive readings and fostered the creation of nanovesicles endowed with superior stability. The identity of the lipid (X4) also emerged as a highly significant determinant of Z.P. values ($P < 0.0001$); all SPC-based formulations devoid of cationic surfactant returned negative Z.P. readings, a reflection of the arrangement of phosphate moieties directed toward the outer vesicle surface [41]. By contrast, PL-90 G yielded a faintly positive interfacial charge, which may be rationalized by outward leakage of the cationic drug through the comparatively leaky bilayer constituted by unsaturated fatty acid-bearing lipid, bearing in mind that PL-90 G possesses an essentially neutral charge at physiological pH, as discussed previously.

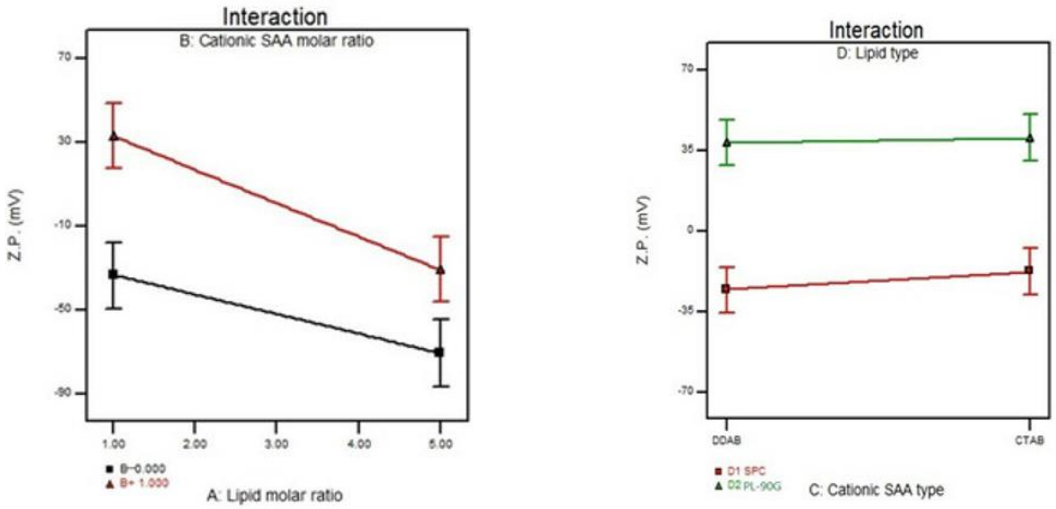

a) b)

Figure 3. The effect of lipid molar ratio (X1), cationic surfactant molar ratio (X2), cationic surfactant type (X3), and lipid type (X4) on Z.P. Abbreviation: Z.P. = zeta potential.

Effect of formulation variables on the in vitro drug release

The in vitro release performance of VAN from the various LPX formulations was characterized using the Jss parameter. Across the tested nanocarrier systems, Jss values ranged from 36.06 ± 0.49 to 187.41 ± 1.2 μg/cm²/h, as shown in **Table 2**. ANOVA results showed that X1, X2, X3, and X4 each had a significant effect on the release kinetics of the prepared LPX, as depicted in **Figure 4**. Augmenting the lipid proportion was accompanied by a decline in Jss, a phenomenon attributable to diminished bilayer deformability, a gain in vesicle stiffness, and a concomitant thickening of the medium. These collective alterations may act to retard drug migration into the dissolution milieu [29]. In opposition to this trend, raising the surfactant fraction corresponded with an elevation in Jss values, perhaps a consequence of the production of finer vesicles that collectively furnish a more expansive interfacial region for drug liberation. Swapping the more hydrophobic surfactant DDAB (log P 11.8) for the somewhat less hydrophobic CTAB (log P 8) suppressed the observed Jss. The selection of lipid type (X4) further modulated the Jss, with PL-90 G consistently delivering greater flux than SPC. This discrepancy is plausibly grounded in the contrasting levels of fatty acid saturation between PL-90 G and SPC. These findings are consonant with those of Parmar *et al*. [42], who established that the release pattern of a drug from lipid-based nanocarriers was contingent upon the extent of saturation inherent to the phospholipid deployed during preparation, as bilayer permeability is heavily swayed by its molecular makeup; the presence of saturated phospholipid species within the bilayer matrix fortifies its structural rigidity and, correspondingly, throttles the fraction of drug discharged.

Based on the computed regression coefficients, the release profiles of all LPX formulations most closely conformed to the Higuchi kinetic model.

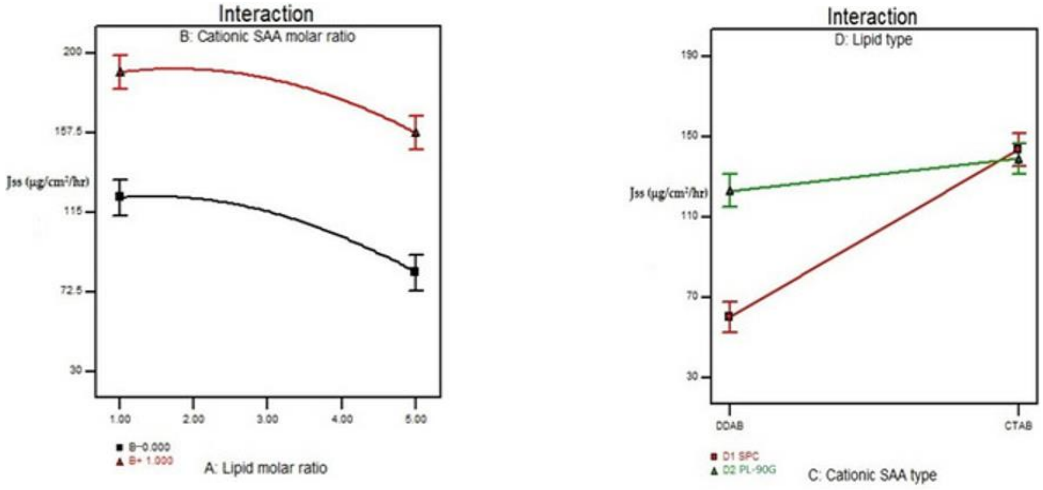

a) b)

Figure 4. The effect of lipid molar ratio (X1), cationic surfactant molar ratio (X2), cationic surfactant type (X3), and lipid type (X4) on Jss—abbreviation: Jss = steady-state flux.

Selection of the optimized LPX formula

The process of pinpointing the best-performing LPX composition involved specifying a set of target constraints in Design Expert® version 7. The imposed optimization goals favored nanovesicles with the highest E.E.%, Z.P., and Jss, and the lowest P.S. and P.I. values. The candidate that satisfied all predefined benchmarks was formulated with CTAB as the cationic surfactant and PL-G 90 as the lipid backbone, combined at a molar ratio of 1:0.67. The composite desirability rating for this lead formulation amounted to 0.802, and its experimentally determined characteristics were as follows: E.E.% of 85.2 ± 0.95%, P.S. of 52.74 ± 0.91 nm, P.I. of 0.21 ± 0.02, Jss of 175.03 ± 1.68 µg/cm²/h, and Z.P. of 60.8 ± 1.75 mV. **Table 3** presents the model-forecasted and empirically observed response values for the selected formulation, showing tight alignment between the two.

Morphology of the optimized LPX formula

TEM imaging of the LPX architecture revealed spherical entities with a homogeneous diameter distribution. The size bracket estimated from electron micrographs was in close agreement with that measured by the Zetasizer, as shown in **Figure 5.**

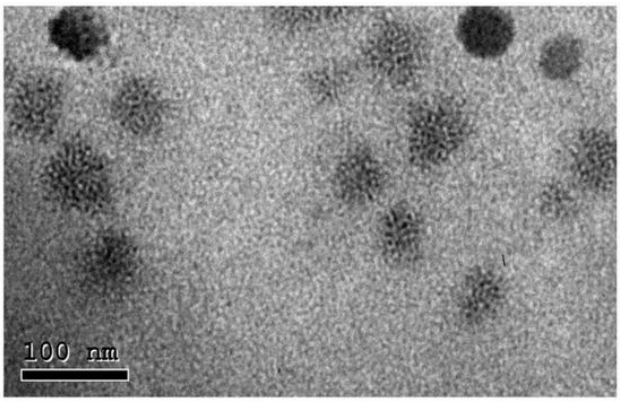

Figure 5. Morphology of the selected LPX. Abbreviation: LPX = leciplex.

Ex Vivo permeation study

The total amount of VAN that penetrated across the gut wall after the 8 h experimental window (Q8) proved to be considerably greater (unpaired t-test, $p < 0.05$) for the optimized LPX dispersion, achieving 404.62 ± 1.95

µg/cm², in contrast to a mere 178.74 ± 1.75 µg/cm² for the drug in its free solution state, according to the data collated in **Table 4 and Figure 6**. A key contributor to this effect may be the extremely fine P.S. of the LPX carrier (52.74 ± 0.91 nm), which endows the system with an enlarged interfacial territory favorable for absorptive processes. Moreover, the net electropositive character of the nanovesicle surfaces promotes firm adhesion to the electronegative exterior of epithelial cells. This interaction extends the temporal window for uptake and promotes inward vesicle trafficking via endocytosis [43]. An additional mechanism involves the incorporated surfactant, which can disorder the structural packing of the cell membrane lipid bilayer, thereby facilitating drug entry and loosening intercellular tight junction complexes that link neighboring epithelial cells. Across the work presented here, the LPX carrier boosted the apparent permeability coefficient of VAN by a multiplicative factor of 2.3 relative to the untreated drug solution.

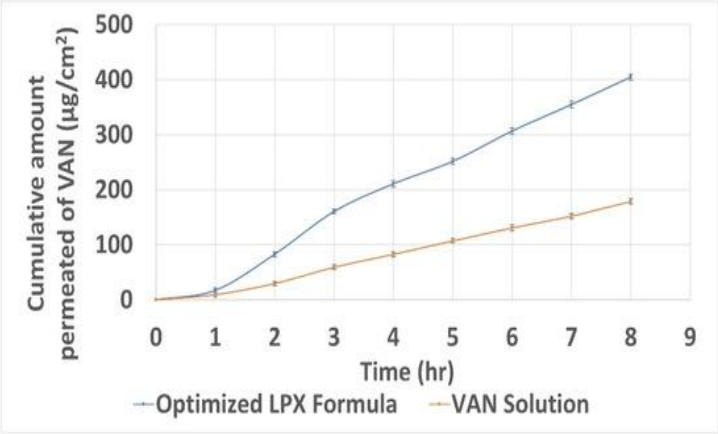

Figure 6. Cumulative amount permeated of VAN from the optimized LPX formula and aqueous solution. Abbreviations: VAN, Vancomycin hydrochloride; LPX, leciplex.

Table 4. Intestinal permeability parameters of VAN after application of VAN solution and LPX.

Intestinal permeability parameters	VAN solution	LPX
Total amount of VAN permeated per unit area after 8 hours (µg/cm²)	178.74 ± 1.75	404.62 ± 1.95
Apparent permeability (cm/h)	0.00970 ± 0.0004	0.2240 ± 0.0007

Differential scanning calorimetry

To garner supplementary evidence for intermolecular associations between VAN and the individual LPX building blocks, DSC thermal scans were collected for VAN, PL-90 G, CTAB, and the finalized LPX system, as collated in **Figure 7.** The thermal trace for neat VAN was dominated by a single, somewhat diffuse endothermic event peaking at 83.4 °C, diagnostic of the compound's melting transition. The scan for PL-90 G showed three moderately broad endothermic excursions at 146, 174, and 265 °C. The thermogram from CTAB showed two sharply defined endothermic valleys within the examined temperature range at 102.4 °C and 261 °C. Turning to the LPX specimen, three endothermic transitions were captured at 111, 149, and 232 °C. The migration of the PL-90 G-associated endotherms toward cooler temperature coordinates can reasonably be attributed to the molecular-level dissolution of PL-90 G by CTAB. Such an alteration lends credence to the notion of a physicochemical interplay between the cationic surfactant and the phospholipid constituent of the LPX architecture. Equally telling was the total effacement of the diagnostic VAN fusion peak, an indication that the drug cargo had been exhaustively enclosed within the cationic nanocarrier matrix. These observations are consistent with the account given by Beg *et al*. [44], who described how the extinction of the semi-ordered crystalline features of rosuvastatin in DSC thermograms substantiated its accommodation within phospholipid-anchored nanolipospheres, driven by hydrogen bonding and van der Waals forces between the drug and PL-90 G.

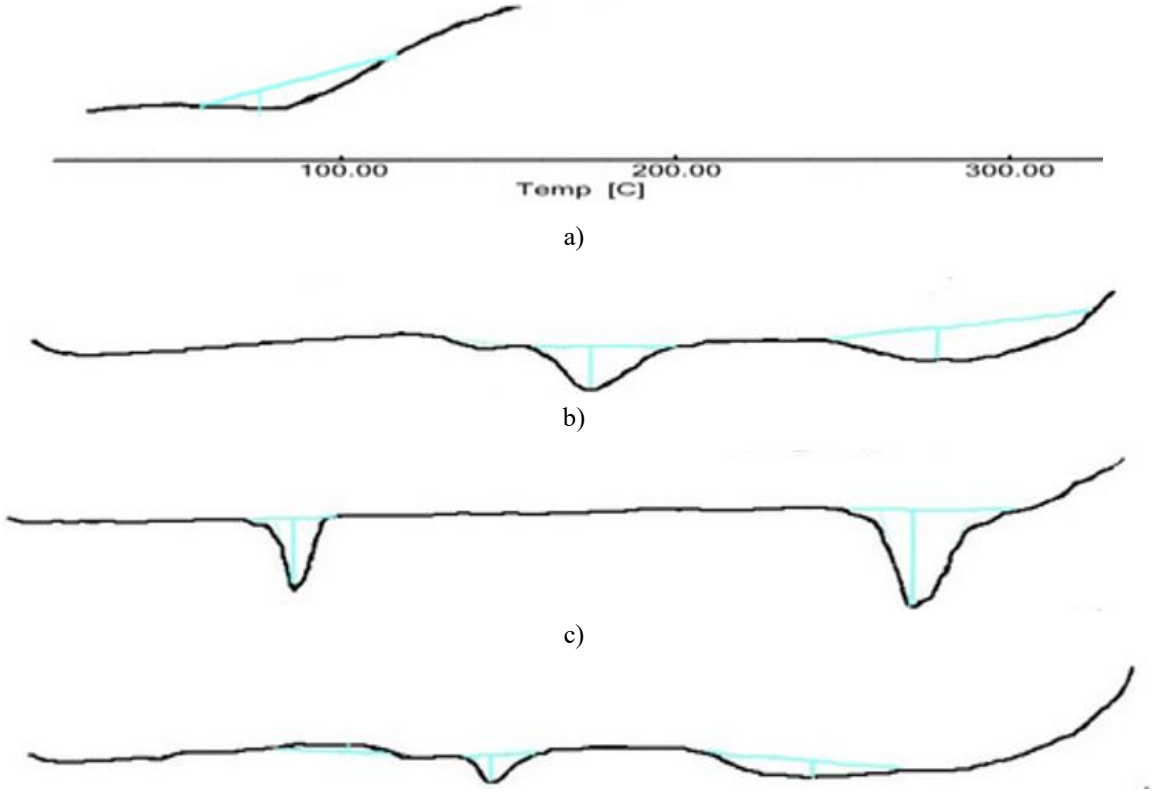

Figure 7. DSC thermograms: a, VAN; b, PL-90 G; c, CTAB; d, LPX formula. Abbreviations: DSC = differential scanning calorimetry; VAN = vancomycin hydrochloride; PL-90 G = phospholipon 90 G; CTAB = cetyltrimethylammonium bromide; LPX = leciplex.

Effect of storage on the selected LPX formula

The kinetic physical stability of lipid-based vesicular dispersions varies inversely with particle diameter and scales directly with the absolute Z.P. of the system. Clustering of vesicles, a hallmark of compromised dispersion integrity, may manifest either during the manufacturing workflow or across the shelf-life period. Gross visual scrutiny of the LPX specimen over the storage term revealed neither the formation of settled deposits nor any signs of vesicle flocculation. Correspondingly, the reassessed parameters—E.E.% standing at 84.6 ± 0.41%, P.S. at 54.94 ± 0.97 nm, P.I. at 0.267 ± 0.03, and Z.P. at 60.6 ± 0.41 mV—showed no meaningful divergence from the baseline values of the freshly fabricated LPX (paired t-test, $P > 0.05$). Viewed as a whole, these data underscore the colloidal stability of the prepared LPX, a property plausibly conferred by the CTAB component, which blankets the nanocarrier surface with a dense positive charge. The electrical character of nanovesicles is a cornerstone attribute that governs vesicular behavior; reciprocal electrostatic repulsive forces effectively deter vesicle approach and coalescence, thereby safeguarding vesicle stability [30]. The robustness of VAN against the corrosive biochemical environment of the GIT is a decisive factor in any strategy aimed at enhancing its oral bioavailability, as underscored by Uhl *et al*. [45], who demonstrated a direct correlation between improved oral absorption of VAN and its enhanced stability when encapsulated in tetraether lipid liposomes. Quantification of the VAN fraction remaining associated with the LPX carrier following challenge with SGF and SIF yielded 85.2% ± 1.67% and 92.6% ± 0.98%, respectively, figures that affirm the cationic LPX platform's capacity to withstand the inhospitable gastric and intestinal biochemical environments. These outcomes are reminiscent of those reported by Date *et al*. [23], who theorized that LPX could insulate quercetin from enzyme-mediated breakdown within the GIT, thereby delivering a greater fraction of the encapsulated payload into the systemic circulation.

Evaluation of mucoadhesion properties

Upon the introduction of mucin to the cationic nanocarrier dispersion, a reversal in the sign of the interfacial charge was recorded, shifting from the baseline electronegative reading of mucin alone (−9.58 mV ± 0.53) into the electropositive territory (+9.09 mV ± 0.54). This flipping of charge polarity was fully expected as a direct

result of electrostatic complexation between the anionic mucin glycoproteins and the cationic nanocarrier (LPX) and stands as compelling proof of the mucoadhesive disposition inherent to the LPX system. Mucoadhesion of this nature equips the carrier to tether itself firmly to the mucosal wall, thereby protracting the residence period within the gut and accordingly magnifying the extent of drug absorption [46].

Cytotoxicity assay

The in vitro biocompatibility, gauged through the percentage of surviving cells, was determined for the LPX dispersion, the unformulated drug solution, and a cytotoxic reference agent (Cis-Platin) employing the procedure outlined in the methodological section. As set out in **Figure 8**, the proportion of viable cells recorded for the LPX test samples remained statistically on par with that of the plain drug solution at every dosing level examined (unpaired t-test, $P > 0.05$). This result indicates that the LPX formulation is biologically tolerable and thus appropriate for oral drug-delivery applications. Such a conclusion is of considerable importance, given that numerous publications have flagged the inherent cytotoxicity of cationic surfactants; however, it must be noted that this toxic effect is dose-dependent and typically subsides markedly once the surfactant becomes intercalated within a lipid bilayer [29].

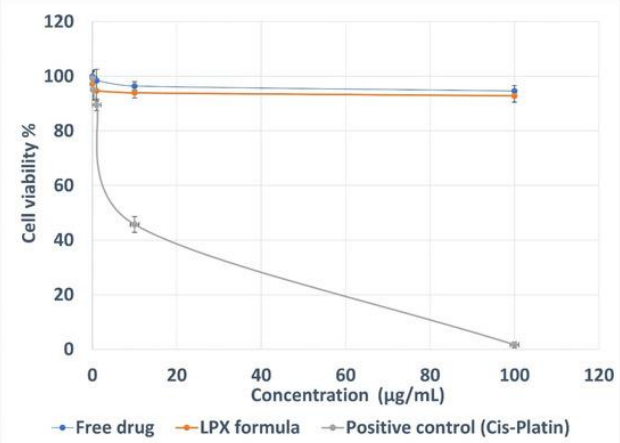

Figure 8. Cell viability percent using SRB colorimetric assay—abbreviation: SRB = sulforhodamine B.

In Vivo assessment of the selected LPX formula

Depicted in **Figure 9** are the plasma drug concentration–time graphs belonging to the optimal LPX preparation set alongside those of the VAN solution, both obtained after oral gavage in the rat subjects. VAN delivered through the LPX carrier achieved a Cmax that proved markedly higher (unpaired t-test, $P < 0.05$), exhibiting a 2.99-fold rise (Cmax, 200.54 ± 2.53 µg/mL) when contrasted with the aqueous VAN dispersion (Cmax, 67.00 ± 1.95 µg/mL). The time coordinates at which peak plasma levels were observed were 5 h for the LPX group and 4 h for the control solution. This rightward shift in Tmax associated with the LPX construct implies an inherent capacity for prolonged drug liberation. The integrated AUC0–t amounted to 1969.54 ± 2.63 µg·h/mL for the nanocarrier cohort, whereas the corresponding value was merely 576.11 ± 1.21 µg·h/mL for the unformulated drug. Computation of MRT yielded values of 44.13 ± 1.83 h and 19.5 ± 1.28 h for the LPX system and the reference solution, respectively.

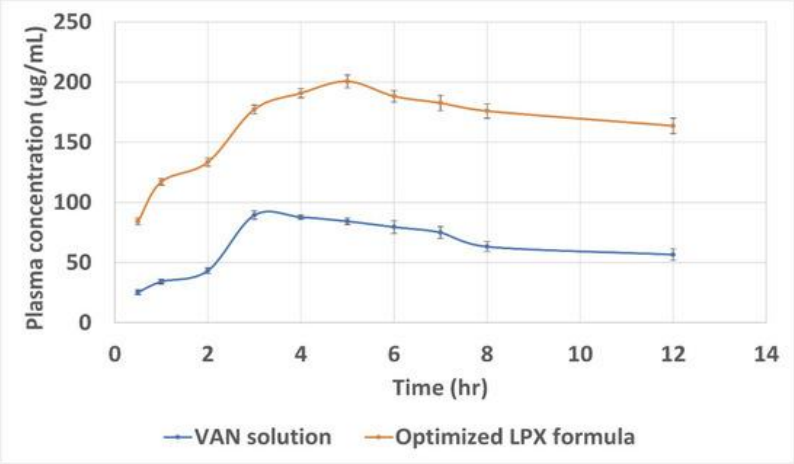

Figure 9. Mean plasma concentration-time curve of VAN following oral administration of the optimized LPX formula and VAN aqueous solution—abbreviation: VAN = vancomycin hydrochloride; LPX = leciplex.

The movement of pharmaceutical compounds across the gut epithelial lining is an intricate, dynamic phenomenon orchestrated by multiple distinct transport pathways and cellular processes. Pinpointing a single dominant mode of permeation is, for this reason, inherently difficult. That said, the superior intestinal assimilation of VAN realized through the LPX platforms can be interpreted by reference to a series of mutually reinforcing contributors: (a) the shielding afforded to VAN molecules sequestered within the LPX core, insulating them from the corrosive biochemical conditions of the stomach; (b) the synchronized delivery of bio-enhancer excipients and the therapeutic payload together at the locus of absorption; (c) the capacity of the bio-enhancer to remodel the permeability characteristics of the intestinal mucosa, thus accelerating VAN transit across the gastric barrier through both transcellular and paracellular avenues; (d) the mucus-anchoring tendency of LPX, which prolongs its retention within the GIT, sustains intimate apposition between the carrier and the villous epithelium, and accordingly broadens the temporal opportunity for oral drug uptake—whether the VAN remains vesicle-bound or exists in free form—relative to the simple solution, ultimately translating into amplified passive diffusion across the intestinal boundary; and (e) the ultra-fine particle caliber together with the attendant expansive specific surface area intrinsic to the LPX dispersion.

The magnitude of oral bioavailability enhancement attainable for a water-soluble macromolecule entrapped within lipid-based vesicles is critically governed by the trajectory those vesicles follow once they enter the alimentary canal, with vesicular robustness during GIT transit representing a factor of paramount importance. Among the orally ingested lipid vesicles, one portion is demolished by the strongly acidic gastric environment. In contrast, those that endure this initial challenge proceed into the duodenum and jejunum, where intestinal bile salts and luminal hydrolases eradicate a further subset. The minor fraction that persists through these sequential assaults ultimately engages in direct interfacial contact with the gut epithelium and serves as the primary driver of improved oral bioavailability for hydrophilic macromolecular therapeutic agents [47]. The net cationic surface charge of LPX may confer some resistance to GIT-mediated destructive pathways, thereby contributing to the overall elevation of VAN oral bioavailability. In this context, Elnaggar *et al*. [48] demonstrated that positively charged bilosomes designed to boost the oral absorption of the hydrophilic bisphosphonate risedronate were demonstrably more resilient in SGF than their negatively charged analogs, proposing that the considerable electropositive potential retained at low pH would foster strong mutual repulsion between the cationic vesicle population and the approaching acidic species.

The contribution of the cationic surfactant functioning as a bio-enhancer toward augmenting VAN intestinal uptake can be dissected into several discrete yet interrelated actions: (a) disruption of the ordered packing of the cellular phospholipid bilayer, which eases the ingress of drug molecules after their release; (b) disengagement of epithelial tight junction strands, facilitating paracellular permeation of the freed drug; (c) stimulation of vesicle internalization through the endocytic machinery. Observations of a parallel nature were put forward by Parmentier *et al*. [49], whose work centered on potentiating the oral delivery of fluorescein isothiocyanate (FITC)-dextran, a model hydrophilic macromolecule, via liposomal carriers outfitted with assorted bio-enhancers, including cetylpyridinium chloride and cholylsarcosine, in conjunction with stearylamine. Their data established that the

cationic surfactant cetylpyridinium chloride significantly outperformed the other permeation promoters in raising the oral bioavailability of FITC-dextran, an effect mediated jointly through heightened cellular internalization (transcellular arm) and loosening of tight junction barriers (paracellular arm), prompting the conclusion that both mechanistic routes are conceivably operational for this particular formulation strategy. In addition to the foregoing, the cationic surfactant engendered electrostatic bonding between the LPX particles and the mucus blanket, thereby strengthening the mucoadhesive tethering of the LPX nanoparticles. This interaction would plausibly prolong the gastrointestinal sojourn, sustain drug delivery to the underlying epithelial interface, elevate local drug concentration at the absorption front, and thereby magnify VAN uptake. Prolonged gastrointestinal persistence of the lipid vesicles also amplifies the statistical probability of their recognition and engulfment by M cells [24]. Yi *et al*. [50] moreover articulated the concept that mucoadhesive association with epithelial cells potentiates the endocytic entrapment of nanovesicles, considering that the process of epithelial membrane wrapping around a nanoparticle is fundamentally dependent on the adhesive interplay between the two surfaces.

It has long been recognized that a reduction in P.S. is an essential design feature for promoting gastrointestinal uptake via both endocytic and paracellular mechanisms. A substantial body of published systematic investigations has examined the determinants of cellular internalization efficiency, identifying nanoparticle attributes, such as diameter, surface chemistry, and overall morphology, as influential factors. A consensus holds that the minimal membrane-wrapping time is governed principally by the particle radius [51, 52]. Extending this reasoning, Delon *et al*. [53] observed that paracellular transit permits solely the movement of entities possessing sufficiently small dimensions. Furthermore, the sub-micron size range affords a dramatically enlarged interfacial area available for absorptive phenomena [54]. Despite the numerically modest representation of M cells in the intestinal lining, this particular transport corridor may nonetheless contribute to enhanced VAN gut permeability attributable to the reduced P.S. These conclusions resonate with the findings of Daeihamed *et al*. [55], who noted that liposomal particle size could similarly modulate uptake efficiency via M cells located within Peyer's patches.

The phospholipid constituent embedded within the LPX architecture exhibits both water-attracting and lipid-attracting domains. This duality closely mirrors the amphiphilic nature of the phospholipid bilayer that composes human cellular membranes. This property gives LPX a distinctive edge in permeability enhancement, as it promotes more intimate molecular-level contact between the drug substance and the cell membrane. Permeability amplification observed with phospholipid-centric delivery platforms has been ascribed to a single mechanism or, more commonly, to the convergence of four principal mechanisms: surface adsorption, endocytic engulfment, direct membrane fusion, and intermembrane lipid exchange [26].

Taken together, the lipid-anchored nanocarrier LPX platform significantly increased the oral bioavailability of a high-molecular-mass pharmaceutical agent belonging to BCS class III; these results are consistent with the body of earlier literature that has exploited lipid-based nanocarrier technologies to enhance the oral delivery performance of water-soluble drugs [56, 57].

Conclusion

The potential of cationic nanocarriers embodied as leciplex (LPX) to raise the oral bioavailability of a macromolecular drug characterized by high aqueous solubility yet restricted permeability (VAN) was conclusively demonstrated. A multiplicity of likely interwoven mechanisms may have acted in concert to produce the measured gain in VAN oral bioavailability, encompassing protection from enzymatic digestion in the GIT, the co-presence of a bio-enhancer agent, nanometer-scale particle dimensions, and mucoadhesive surface characteristics. The molar proportions of the lipid and cationic surfactant building blocks, as well as their specific chemical natures, were additionally shown to exert a commanding influence over the ultimate attributes of the formulated LPX. Future research is necessary to disentangle the exact mechanistic pathways underlying LPX-mediated improvements in the oral bioavailability of hydrophilic macromolecular compounds.

Acknowledgments: None

Conflict of Interest: None

Financial Support: None

Ethics Statement: The animal study protocol was approved by the Ethics Committee of the Faculty of Pharmacy, Cairo University (Approval NO.PI 2842, 28 December 2020).

References

1. Maher S, Geoghegan C, Brayden DJ. Intestinal permeation enhancers to improve oral bioavailability of macromolecules: Reasons for low efficacy in humans. Expert Opin Drug Deliv. 2021;18:273-300.
2. Gamboa A, Schüßler N, Soto-Bustamante E, Romero-Hasler P, Meinel L, Morales JO. Delivery of ionizable hydrophilic drugs based on pharmaceutical formulation of ion pairs and ionic liquids. Eur J Pharm Biopharm. 2020;156:203-18.
3. Phan TNQ, Shahzadi I, Bernkop-Schnürch A. Hydrophobic ion-pairs and lipid-based nanocarrier systems: The perfect match for delivery of BCS class 3 drugs. J Control Release. 2019;304:146-55.
4. Deng F, Bae YH. Bile acid transporter-mediated oral drug delivery. J Control Release. 2020;327:100-16.
5. Homayun B, Lin X, Choi HJ. Challenges and recent progress in oral drug delivery systems for biopharmaceuticals. Pharmaceutics. 2019;11:129.
6. Xu Y, Shrestha N, Préat V, Beloqui A. An overview of in vitro, ex vivo and in vivo models for studying the transport of drugs across intestinal barriers. Adv Drug Deliv Rev. 2021;175:113795.
7. Xu Y, Shrestha N, Préat V, Beloqui A. Overcoming the intestinal barrier: A look into targeting approaches for improved oral drug delivery systems. J Control Release. 2020;322:486-508.
8. Zhu Q, Chen Z, Paul PK, Lu Y, Wu W, Qi J. Oral delivery of proteins and peptides: Challenges, status quo and future perspectives. Acta Pharm Sin B. 2021;11:2416-48.
9. Dünnhaupt S, Kammona O, Waldner C, Kiparissides C, Bernkop-Schnürch A. Nano-carrier systems: Strategies to overcome the mucus gel barrier. Eur J Pharm Biopharm. 2015;96:447-53.
10. Ye C, Chi H. A review of recent progress in drug and protein encapsulation: Approaches, applications and challenges. Mater Sci Eng C. 2018;83:233-46.
11. Parmentier J, Hofhaus G, Thomas S, Cuesta LC, Gropp F, Schröder R, et al. Improved oral bioavailability of human growth hormone by a combination of liposomes containing bio-enhancers and tetraether lipids and omeprazole. J Pharm Sci. 2014;103:3985-93.
12. Ndayishimiye J, Cao Y, Kumeria T, Blaskovich MA, Falconer JR, Popat A. Engineering mesoporous silica nanoparticles towards oral delivery of vancomycin. J Mater Chem B. 2021;9:7145-66.
13. Cerchiara T, Abruzzo A, Parolin C, Vitali B, Bigucci F, Gallucci MC, et al. Microparticles based on chitosan/carboxymethylcellulose polyelectrolyte complexes for colon delivery of vancomycin. Carbohydr Polym. 2016;143:124-30.
14. Loveymi BD, Jelvehgari M, Zakeri-Milani P, Valizadeh H. Design of vancomycin RS-100 nanoparticles in order to increase the intestinal permeability. Adv Pharm Bull. 2012;2:43-56.
15. Zakeri-Milani P, Loveymi BD, Jelvehgari M, Valizadeh H. The characteristics and improved intestinal permeability of vancomycin PLGA-nanoparticles as colloidal drug delivery system. Colloids Surf B Biointerfaces. 2013;103:174-81.
16. Zaichik S, Steinbring C, Caliskan C, Bernkop-Schnürch A. Development and in vitro evaluation of a self-emulsifying drug delivery system (SEDDS) for oral vancomycin administration. Int J Pharm. 2019;554:125-33.
17. Efiana NA, Dizdarević A, Huck CW, Bernkop-Schnürch A. Improved intestinal mucus permeation of vancomycin via incorporation into nanocarrier containing papain-palmitate. J Pharm Sci. 2019;108:3329-39.
18. Uhl P, Sauter M, Hertlein T, Witzigmann D, Laffleur F, Hofhaus G, et al. Overcoming the mucosal barrier: Tetraether lipid-stabilized liposomal nanocarriers decorated with cell-penetrating peptides enable oral delivery of vancomycin. Adv Ther. 2021;4:2000247.
19. Maher S, Mrsny RJ, Brayden DJ. Intestinal permeation enhancers for oral peptide delivery. Adv Drug Deliv Rev. 2016;106:277-319.
20. Velpula A, Jukanti R, Janga KY, Sunkavalli S, Bandari S, Kandadi P, et al. Proliposome powders for enhanced intestinal absorption and bioavailability of raloxifene hydrochloride: Effect of surface charge. Drug Dev Ind Pharm. 2013;39:1895-906.

21. Babadi D, Dadashzadeh S, Osouli M, Daryabari MS, Haeri A. Nanoformulation strategies for improving intestinal permeability of drugs: A more precise look at permeability assessment methods and pharmacokinetic properties changes. J Control Release. 2020;321:669-709.
22. Kamel R, El-Deeb NM, Abbas H. Development of a potential anti-cancer pulmonary nanosystem consisted of chitosan-doped LeciPlex loaded with resveratrol using a machine learning method. J Drug Deliv Sci Technol. 2022;70:103259.
23. Date AA, Nagarsenker MS, Patere S, Dhawan V, Gude RP, Hassan PA, et al. Lecithin-based novel cationic nanocarriers (LeciPlex) II: Improving therapeutic efficacy of quercetin on oral administration. Mol Pharm. 2011;8:716-26.
24. He H, Lu Y, Qi J, Zhu Q, Chen Z, Wu W. Adapting liposomes for oral drug delivery. Acta Pharm Sin B. 2019;9:36-48.
25. Cuomo F, Ceglie S, Miguel M, Lindman B, Lopez F. Oral delivery of all-trans retinoic acid mediated by liposome carriers. Colloids Surf B Biointerfaces. 2021;201:111655.
26. Dave VS, Gupta D, Yu M, Nguyen P, Varghese Gupta S. Current and evolving approaches for improving the oral permeability of BCS class III or analogous molecules. Drug Dev Ind Pharm. 2017;43:177-89.
27. Romes NB, Wahab RA, Abdul Hamid M, Hashim SE. D-optimal design-assisted Elaeis guineensis leaves extract in olive oil-sunflower seed nanoemulsions: Development, characterization, and physical stability. J Dispers Sci Technol. 2022;43:289-301.
28. Bhattacharya S. Design and development of docetaxel solid self-microemulsifying drug delivery system using principal component analysis and D-optimal design. Asian J Pharm. 2018;12:S122-S144.
29. Hassan DH, Abdelmonem R, Abdellatif MM. Formulation and characterization of carvedilol Leciplex for glaucoma treatment: In vitro, ex vivo and in vivo study. Pharmaceutics. 2018;10:197.
30. Albash R, Abdellatif MM, Hassan M, Badawi NM. Tailoring terpesomes and Leciplex for the effective ocular conveyance of moxifloxacin hydrochloride (comparative assessment): In vitro, ex vivo, and in vivo evaluation. Int J Nanomedicine. 2021;16:5247-63.
31. Abdellatif MM, Josef M, El-Nabarawi MA, Teaima M. Sertaconazole nitrate-loaded Leciplex for treating keratomycosis: Optimization using D-optimal design and in vitro, ex vivo, and in vivo studies. Pharmaceutics. 2022;14:2215.
32. Fong SYK, Martins SM, Brandl M, Bauer-Brandl A. Solid phospholipid dispersions for oral delivery of poorly soluble drugs: Investigation into celecoxib incorporation and solubility-in vitro permeability enhancement. J Pharm Sci. 2016;105:1113-23.
33. Lavanya N, Muzib YI, Aukunuru J, Balekari U. Preparation and evaluation of a novel oral delivery system for low molecular weight heparin. Int J Pharm Investig. 2016;6:148-57.
34. Allam RM, Al-Abd AM, Khedr A, Sharaf OA, Nofal SM, Khalifa AE, et al. Fingolimod interrupts the cross talk between estrogen metabolism and sphingolipid metabolism within prostate cancer cells. Toxicol Lett. 2018;291:77-85.
35. Prasad YVR, Puthli SP, Eaimtrakarn S, Ishida M, Yoshikawa Y, Shibata N, et al. Enhanced intestinal absorption of vancomycin with Labrasol and d-α-tocopheryl PEG 1000 succinate in rats. Int J Pharm. 2003;250:181-90.
36. Date AA, Srivastava D, Nagarsenker MS, Mulherkar R, Panicker L, Aswal V, et al. Lecithin-based novel cationic nanocarriers (LeciPlex) I: Fabrication, characterization and evaluation. Nanomedicine. 2011;6:1309-25.
37. Salama A, Badran M, Elmowafy M, Soliman GM. Spironolactone-loaded LeciPlexes as potential topical delivery systems for female acne: In vitro appraisal and ex vivo skin permeability studies. Pharmaceutics. 2020;12:25.
38. Eroğlu İ, Azizoğlu E, Özyazıcı M, Nenni M, Gürer Orhan H, Özbal S, et al. Effective topical delivery systems for corticosteroids: Dermatological and histological evaluations. Drug Deliv. 2016;23:1502-13.
39. Therdphapiyanak N, Jaturanpinyo M, Waranuch N, Kongkaneramit L, Sarisuta N. Development and assessment of tyrosinase inhibitory activity of liposomes of Asparagus racemosus extracts. Asian J Pharm Sci. 2013;8:134-42.
40. Khatoon K, Rizwanullah M, Amin S, Mir SR, Akhter S. Cilnidipine loaded transfersomes for transdermal application: Formulation optimization, in vitro and in vivo study. J Drug Deliv Sci Technol. 2019;54:101303.

41. Ammar HO, Tadros MI, Salama NM, Ghoneim AM. Ethosome-derived invasomes as a potential transdermal delivery system for vardenafil hydrochloride: Development, optimization and application of physiologically based pharmacokinetic modeling in adults and geriatrics. Int J Nanomedicine. 2020;15:5671-85.
42. Parmar JJ, Singh DJ, Hegde DD, Lohade AA, Soni PS, Samad A, et al. Development and evaluation of inhalational liposomal system of budesonide for better management of asthma. Indian J Pharm Sci. 2010;72:442-8.
43. Cao SJ, Xu S, Wang HM, Ling Y, Dong J, Xia RD, et al. Nanoparticles: Oral delivery for protein and peptide drugs. AAPS PharmSciTech. 2019;20:190.
44. Beg S, Raza K, Kumar R, Chadha R, Katare O, Singh B. Improved intestinal lymphatic drug targeting via phospholipid complex-loaded nanolipospheres of rosuvastatin calcium. RSC Adv. 2016;6:8173-87.
45. Uhl P, Pantze S, Storck P, Parmentier J, Witzigmann D, Hofhaus G, et al. Oral delivery of vancomycin by tetraether lipid liposomes. Eur J Pharm Sci. 2017;108:111-8.
46. Lin YJ, Shatkin JA, Kong F. Evaluating mucoadhesion properties of three types of nanocellulose in the gastrointestinal tract in vitro and ex vivo. Carbohydr Polym. 2019;210:157-66.
47. Sheikholeslami B, Lam NW, Dua K, Haghi M. Exploring the impact of physicochemical properties of liposomal formulations on their in vivo fate. Life Sci. 2022;300:120574.
48. Elnaggar YSR, Omran S, Hazzah HA, Abdallah OY. Anionic versus cationic bilosomes as oral nanocarriers for enhanced delivery of the hydrophilic drug risedronate. Int J Pharm. 2019;564:410-25.
49. Parmentier J, Hartmann FJ, Fricker G. In vitro evaluation of liposomes containing bio-enhancers for the oral delivery of macromolecules. Eur J Pharm Biopharm. 2010;76:394-403.
50. Yi X, Shi X, Gao H. Cellular uptake of elastic nanoparticles. Phys Rev Lett. 2011;107:098101.
51. Xu A, Yao M, Xu G, Ying J, Ma W, Li B, et al. A physical model for the size-dependent cellular uptake of nanoparticles modified with cationic surfactants. Int J Nanomedicine. 2012;7:3547-54.
52. Gossmann R, Langer K, Mulac D. New perspective in the formulation and characterization of didodecyldimethylammonium bromide (DMAB) stabilized poly(lactic-co-glycolic acid) (PLGA) nanoparticles. PLoS One. 2015;10:e0127532.
53. Delon L, Gibson RJ, Prestidge CA, Thierry B. Mechanisms of uptake and transport of particulate formulations in the small intestine. J Control Release. 2022;343:584-99.
54. Bajka BH, Rigby NM, Cross KL, Macierzanka A, Mackie AR. The influence of small intestinal mucus structure on particle transport ex vivo. Colloids Surf B Biointerfaces. 2015;135:73-80.
55. Daeihamed M, Haeri A, Ostad SN, Akhlaghi MF, Dadashzadeh S. Doxorubicin-loaded liposomes: Enhancing the oral bioavailability by modulation of physicochemical characteristics. Nanomedicine. 2017;12:1187-202.
56. Ling SSN, Magosso E, Abdul Karim Khan N, Hay Yuen K, Anne Barker S. Enhanced oral bioavailability and intestinal lymphatic transport of a hydrophilic drug using liposomes. Drug Dev Ind Pharm. 2006;32:335-45.
57. Palassi S, Valizadeh H, Allahyari S, Zakeri-Milani P. Preparation and in vitro characterization of enoxaparin nanoliposomes through different methods. Adv Pharm Bull. 2021;11:295-300.